

Corrosion Prediction for Naphtha and Gas System of Atmospheric Distillation Tower Based on Artificial Neural Network and Genetic Algorithm

Hao Li, Guoming Yang^{*}, Jing Xin, Ying Wu, Guangting Xue

Petroleum Refining Research Institute, China National Offshore Oil Corporation Research, Beijing, China

Email address:

lihao27@cnooc.com.cn (Hao Li), yanggm8@cnooc.com.cn (Guoming Yang)

^{*}Corresponding author

To cite this article:

Hao Li, Guoming Yang, Jing Xin, Ying Wu, Guangting Xue. Corrosion Prediction for Naphtha and Gas System of Atmospheric Distillation Tower Based on Artificial Neural Network and Genetic Algorithm. *International Journal of Oil, Gas and Coal Engineering*. Vol. 6, No. 1, 2018, pp. 25-33. doi: 10.11648/j.ogce.20180602.11

Received: April 26, 2018; Accepted: May 22, 2018; Published: June 19, 2018

Abstract: The corrosion of low-temperature sections of a company's atmospheric and vacuum distillation unit was analyzed. Corrosion rate prediction model was established using BP neural network based on the corrosion detection data detected in the sewage on top of the tower over a period of time. In this model, the pH value, Cl ion concentration, Fe ion concentration and sulfide concentration of the sewage discharged from the top of the tower are taken as the input data, and the average corrosion rate as the output data, the results show that the prediction error is large. The BP neural network was optimized using the genetic algorithm. The optimized model could accurately predict the corrosion of the atmospheric unit at low temperatures. The corrosion rate prediction model was used to investigate the effect of each variable on the corrosion rate through the single factor change and the results could reflect the relationship between detected corrosion data and corrosion rate in the sewage on top of the atmospheric tower.

Keywords: Atmospheric Distillation Tower Corrosion, BP Neural Network, Genetic Algorithm, Corrosion Rate Prediction

1. Introduction

The atmospheric and vacuum distillation unit has a large impact on the overall operation and processing capacity of the refinery as the first processing unit. The crude naphtha is transformed to distillates of different naphthaing ranges by distillation in the unit. Crude naphtha usually contains much Cl ions and sulfur ions, which easily forms a corrosive environment of HCl-H₂S-H₂O at high temperatures, causing corrosion attack on the naphtha and gas system of atmospheric distillation tower. Equipment maintenance and material replacement caused by corrosion waste a lot of resources and shorten the operation cycle of the devices [1]. Therefore, the corrosion prediction for naphtha and gas pipelines on top of atmospheric distillation tower is of great significance to the production and maintenance of the devices.

However, in the actual production environment, the influence of various factors on corrosion is complicated and it is difficult to establish an accurate mathematical model. The

BP neural network can determine the mathematical model for corrosion through its own strong learning ability and multi-factor cooperation ability and predict the corrosion rate. However, the prediction accuracy is low when the data samples are limited, so it is difficult to meet the practical engineering demands. In this paper, the BP neural network was optimized by genetic algorithm, improving the prediction accuracy of corrosion rate and it provides reference for corrosion detection [2].

2. Pipeline Corrosion Factor Analysis and Training Data Source Selection

A company's atmospheric and vacuum unit mainly processes high-acid heavy crude naphtha, and its pipeline on top of atmospheric tower is made of carbon steel. Crude naphtha processing volume is 50t/h, temperature on the top of atmospheric pressure tower is 94-112°C, and pressure is

1.9-13.4kpa.

The reasons for the low-temperature part corrosion of the atmospheric equipment are mainly as follows: 1. The effect of electric desalination is poor leading to the high salt content, and a large amount of chloride floccs to the top of the atmospheric tower and the vacuum tower, forming hydrochloric acid solution with condensate water on the top of the tower causes corrosion of the pipeline [3]. 2. Ammonium injection equipment at the top of the tower is incomplete, which makes it impossible to accurately control the pH value at the top of the tower and it is easy to form HCL-H₂S-H₂O corrosion is easily formed, resulting in a higher concentration of Fe²⁺ ions in the outlet water [4]. 3. The lack of means for detecting the pH value of the condensate water leads to the inability to timely adjust the amount of ammonia injection, making the pH value too low for a long period of time, resulting in long-term acidic corrosion of the atmospheric equipment [5].

Therefore, the pH value, Cl ion concentration, Fe ion concentration, and sulfide concentration of the sewage discharged from the top of the atmospheric tower are selected as training data, and the average corrosion rate is used as the output data.

3. Establishment and Prediction of BP Neural Network Model

The BP neural network selected in this paper has a three-layer structure of input layer, hidden layer and output layer. The main characteristics of multi-layer feedforward neural network are forward transmission of signals and backward transmission of errors [6]. The input signal is processed layer by layer through the input layer and then the hidden layer, output through the output layer. If the output value does not reach the desired output, the error between the output value and the expected value is back propagated, the weight and threshold value of the network are adjusted according to the error, and the error is reduced through repeated multiple iterations until the error is reduced to the permissible value, then the network training is completed. [7].

3.1. Establishment of BP Neural Network

3.1.1. Network Structure Determination

The output data is pH value, Cl ion concentration, Fe ion concentration and sulfide content. Therefore, the number of nodes in the input layer is 4. The selection of nodes number in the hidden layer of the neural network is related to the final prediction accuracy, and the training error decreased with the number of nodes in the hidden layer increasing. Due to overfitting and other reasons, the training error increases with the number of nodes rising in the hidden layer when exceeding a certain scope [8]. Therefore, the approximate range of nodes number in the hidden layer was selected by empirical formula (1). The best effect is obtained when the nodes number of hidden layer is 5 after several experiments. The final output is the corrosion rate, so the nodes number in the output layer is 1. The topology of the neural network is 4-5-1. In this paper, 90

groups of data were randomly selected as training data, and 10 groups were used for network training for predictive data from the 100 sets of data obtained from field tests [9].

$$l < \sqrt{(m+n)} + a \quad (1)$$

In this formula

- n - the number of nodes in the input layer;
- l - the number of nodes in the hidden layer;
- m - the number of nodes in the output layer;
- a - a constant between 0 and 10.

3.1.2. The Determination of Node Transfer Function

In this paper, the tansig function is selected as the training function, in which the output function H of the hidden layer is determined by formula (2), where x is the input variable, w_{ij} is the connection weight number between the input layer and the hidden layer, a is the threshold value of the hidden layer, initialization assignment of the weight and threshold is randomly selected within the interval (0, 1) [10].

$$H_j = f\left(\sum_{i=1}^n w_{ij}x_i - a_j\right) \quad j = 1, 2, \dots, l \quad (2)$$

In this formula

- l - the number of nodes in the hidden layer;
- f - activation function of hidden layer.

The output layer function is the logsig function, and the predicted output O_k of the artificial neural network can be calculated by formula (3).

$$O_k = h\left(\sum_{j=1}^l H_j w_{jk} - b_k\right) \quad k = 1, 2, \dots, m \quad (3)$$

In this formula:

- h - output of the hidden layer;
- W_{jk} - connection weight;
- b - threshold value.

3.1.3. Error Calculation

The network prediction error e is obtained by equation (4).

$$e_k = Y_k - O_k \quad k = 1, 2, \dots, m \quad (4)$$

In this formula:

- O - predicted output;
- Y - Expected output.

3.1.4. Weight Update

The connection weights of the network—w_{ij} and w_{jk} are updated by equations (5) and (6).

$$w_{ij} = w_{ij} + \eta H_j (1 - H_j) x(i) \sum_{k=1}^m w_{jk} e_k \quad (5)$$

$$i = 1, 2, \dots, n; j = 1, 2, \dots, l$$

$$w_{jk} = w_{jk} + \eta H_j e_k \quad j = 1, 2, \dots, l; k = 1, 2, \dots, m \quad (6)$$

In this formula:
 η - learning rate.

3.1.5. Threshold Value Update

The node thresholds of the network a, b are updated by equations (7) and (8).

$$a_j = a_i + \eta H_j (1 - H_j) \sum_{k=1}^m w_{jk} e_k \quad (7)$$

$$j = 1, 2, \dots, l$$

$$b_k = b_k + e_k \quad k = 1, 2, \dots, m \quad (8)$$

In this formula:
e - network prediction error.

3.1.6. Process Determination

Determine if the iteration of the algorithm is complete. If not, returning to step 2.

3.2. Establishment and Prediction of Corrosion Rate Model

In this paper, MATLAB language is used for programming, 90 sets of data are randomly selected as training data, and 10 sets of data are predicted data. It can be seen in Figure 1 that the BP neural network established in this experiment can predict the corrosion of low-temperature parts of atmospheric equipment. Figure 2 shows the absolute error of forecasting results and actual results. The average relative error calculated by absolute error is 21.4%. In this paper, the ratio of the average of the absolute error and the average of the true value is selected as the average relative error, which can reflect the credibility of the measurement. The mean squared error calculated is 2.57%. Mean square error refers to the expected value of the difference between the parameter estimate and the true value of the parameter. The smaller the mean squared error, the better the accuracy of the prediction model to describe the experimental data.

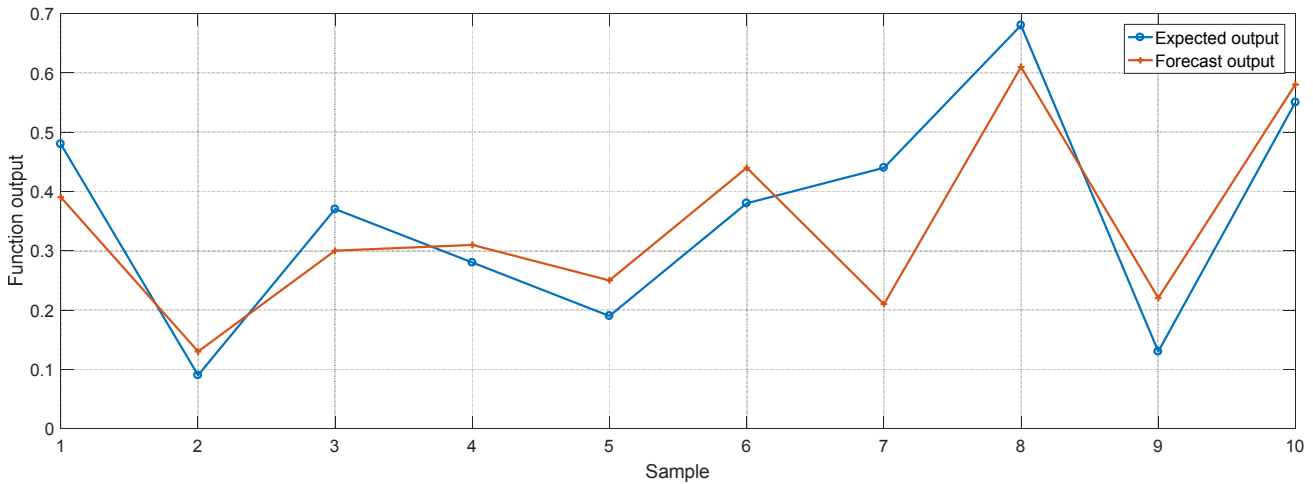


Figure 1. Comparison of predicted output and expected output data of BP neural network.

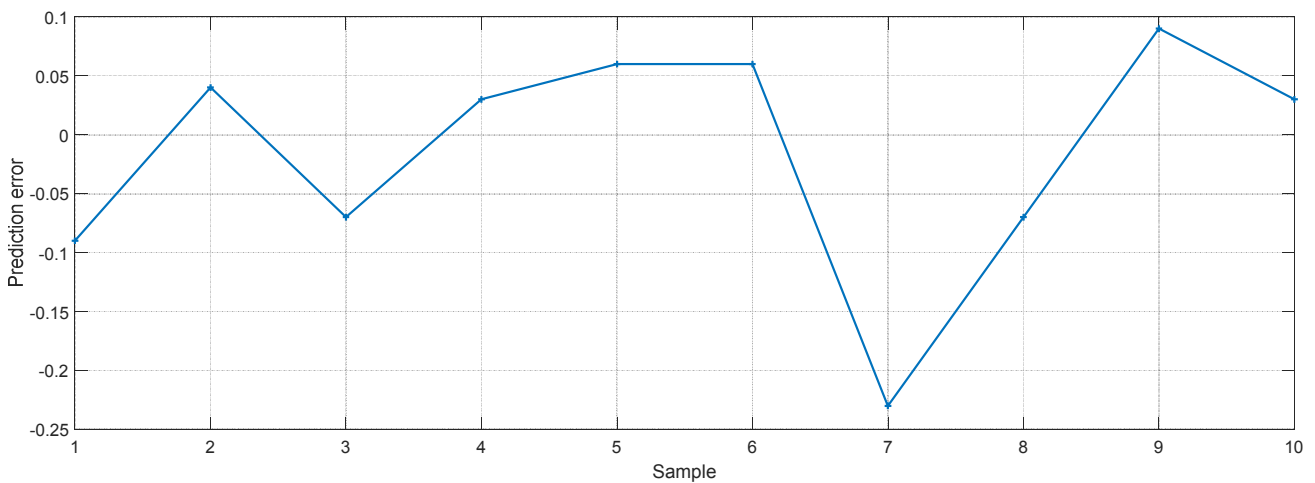


Figure 2. Corrosion rate model prediction error of BP neural network.

The prediction results obtained by BP neural network corrosion are in good conformance with the actual corrosion rate. It shows that the BP neural network has strong learning

ability and forecasting ability, but some individual prediction values diverge largely. The root cause is that the training data is sparse leading the BP neural network not fully trained and

the network prediction value is subject to large errors. In this paper, a genetic algorithm is used to optimize the BP neural network to improve the prediction accuracy.

4. Genetic Algorithm to Optimize BP Neural Network

Genetic algorithm is a parallel stochastic-search optimization method through simulating the natural genetic mechanism and biological evolution theory [11]. According to the selected fitness function, individuals are screened through selection, crossover and mutation in inheritance. Individuals with good fitness values are retained, individuals with poor fitness are eliminated, and new groups inherit the superior information of the previous generation. This cycle will be repeated until the set condition is satisfied. [12]

4.1. Algorithm Flow

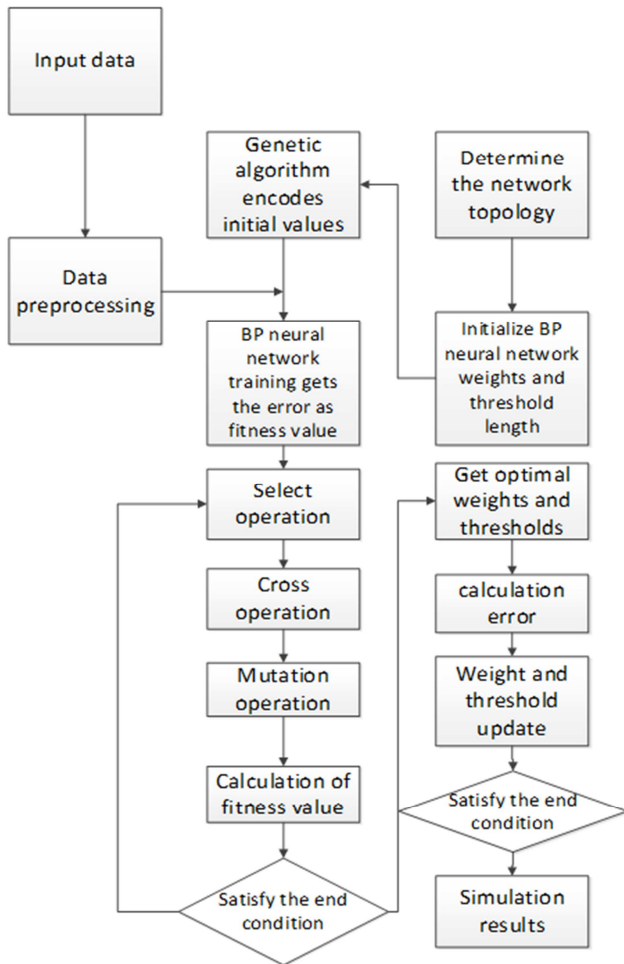


Figure 3. Flow chart of genetic algorithm.

Optimization of BP neural network based on genetic algorithm is to optimize the weights and thresholds of BP neural network by genetic algorithm [13]. Each individual in the population contains all the weights and thresholds of a network. The individual calculates the individual fitness value through the fitness function,

and the genetic algorithm finds out the individuals with optimal fitness value through selection, crossover, and mutation operations. The BP neural network prediction uses the genetic algorithm to obtain the optimal individual and initial network weights and thresholds are assigned, the network predicts the output of the function after being trained [14]. Figure 3 shows the flow chart of the genetic algorithm.

Since the BP neural network structure set in this paper is 4-5-1, that is, the output layer has 4 nodes, the hidden layer has 5 nodes and the output layer has 1 node, with a total of 25 weights and 6 thresholds so the genetic algorithm has an individual code length of 31. Randomly take 90 sets of data as training data and 10 sets of data as prediction data.

4.2. Genetic Algorithm Implementation

The elements of genetic algorithm optimizing BP neural network include population initialization, fitness function, selection operation, crossover operation and mutation operation [15].

4.2.1. Population Initialization

In this paper, all the corrosion data obtained are real strings after being normalized. Therefore, the encoding method selected is real coding, composed by 4 are parts, including the connection weights of the input layer and the hidden layer, the hidden layer threshold, the connection weights of the hidden layer and output layer, and output layer threshold. Combined with the previously established neural network architecture, a complete neural network can be formed.

4.2.2. Fitness Function

The sum E of the absolute error of the output value and the expected value predicted by the neural network is taken as the individual fitness value F, and its fitness can be obtained according to the calculation formula (9)

$$F = k \left(\sum_{i=1}^n abs(y_i - o_i) \right) \tag{9}$$

In this formula:

- n - the number of network output nodes;
- Y_i —the expected output of the I th node of the BP neural network;
- O_i - the predicted output of the I th node;
- K-coefficient

4.2.3. Selection Operation

Based on a real string of samples, fitness-proportionate strategy was selected, namely the roulette method [15]. The selection probability p_i of each individual i is:

$$f_i = k / F_i \tag{10}$$

$$p_i = \frac{f_i}{\sum_{j=1}^N f_j} \tag{11}$$

In this formula:

F_i - the fitness value of individual i ; coefficient;
 N - number of population individuals

4.2.4. Crossover Operation

The K chromosome a_k and L chromosome a_l are crossed at J level by real number crossing method, Methods as below;

$$\begin{aligned} a_{kj} &= a_{kj}(1-b) + a_{lj}b \\ a_{lj} &= a_{lj}(1-b) + a_{kj}b \end{aligned} \tag{12}$$

In this formula:

b - [0-1] random number

4.2.5. Variation Operation

The j -th gene a_{ij} of the i -th individual is mutated as follows

$$a_{ij} = \begin{cases} a_{ij} + (a_{ij} - a_{\max}) \times f(g) & r \gg 0.5 \\ a_{ij} + (a_{\min} - a_{ij}) \times f(g) & r \leq 0.5 \end{cases} \tag{13}$$

In this formula:

a_{\max} - Upper bound of gene a_{ij} ;

a_{\min} - Lower bound of gene a_{ij} ;

$f(g) = r_2(1 - g / G_{\max})^2$;

r_2 - random number;

g - Current iterations;

G_{\max} - Maximum number of evolutions;

r - [0-1] random number

4.3. Genetic Algorithm Optimization BP Neural Network Implementation

In this paper, the BP neural network based on genetic algorithm is applied to predict the corrosion of the overhead naphtha and gas system of atmospheric tower based on genetic algorithm optimized by MATLAB. Through many experiments, the parameter of genetic algorithm is set to: population size 100, Number of evolution 250, The crossover probability is 0.3, The probability of mutation is 0.1.

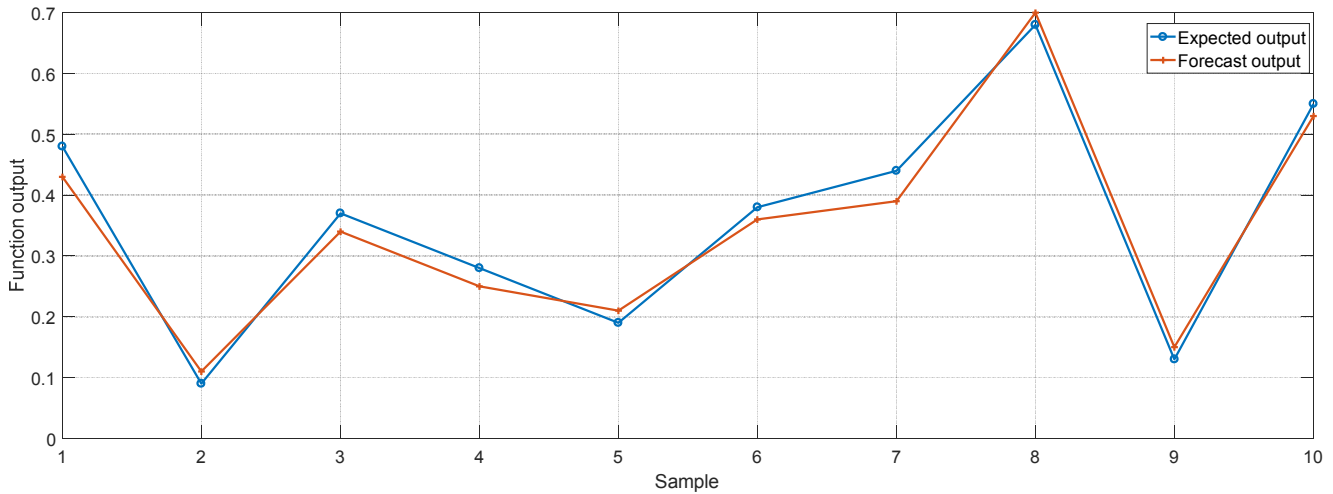


Figure 4. Comparison of prediction output and expected output data of BP neural network optimized by genetic algorithm.

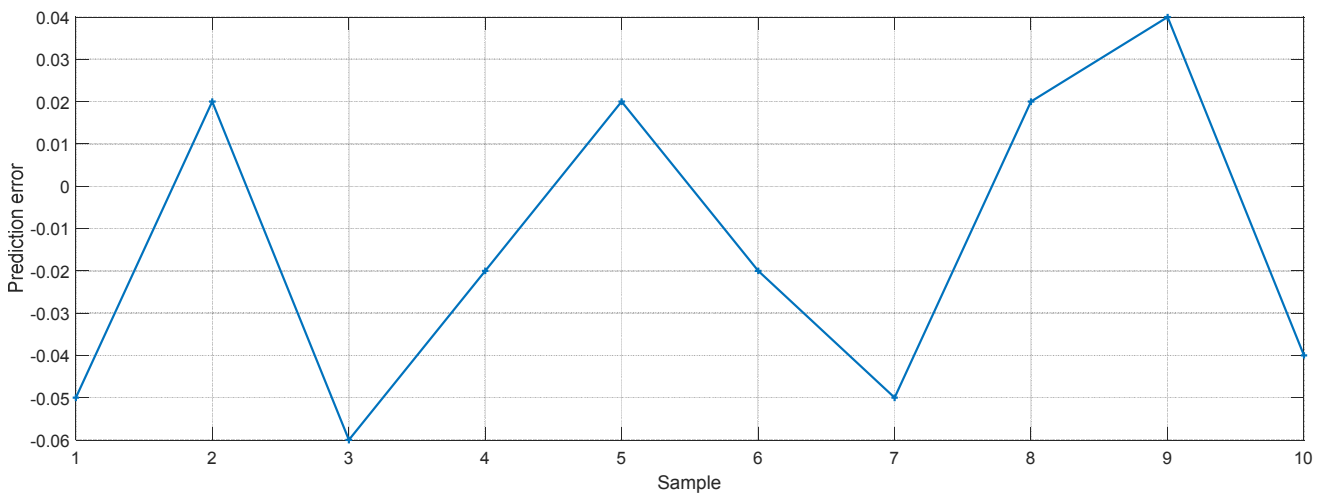


Figure 5. genetic algorithm optimization BP neural network corrosion rate model prediction error.

The forecast result is shown in Figure 4 Corrosion prediction data of BP neural network optimized by genetic

algorithm has higher prediction accuracy, Figure.5 shows the absolute error of the data prediction and actual results, The average relative error calculated by the absolute error is 3.87%, The error value has a certain reduction compared with BP neural network. Calculating the mean square error of 3.03% also has a certain reduction compared with BP neural network. It shows that the performance of the BP neural network after the optimization of the genetic algorithm is higher than that of the non-optimized network, which reflects the better accuracy of the prediction model to describe the experimental data.

5. Corrosion Rate Model Operation

In the actual production environment, Corrosion is caused by a variety of factors. It is difficult to determine the influence of single factor on it, This makes some difficulties in the study of anticorrosion. This article uses the established corrosion prediction model to investigate the effect of various factors on the corrosion rate.

5.1. Influence of Iron Ion Concentration on Corrosion Rate

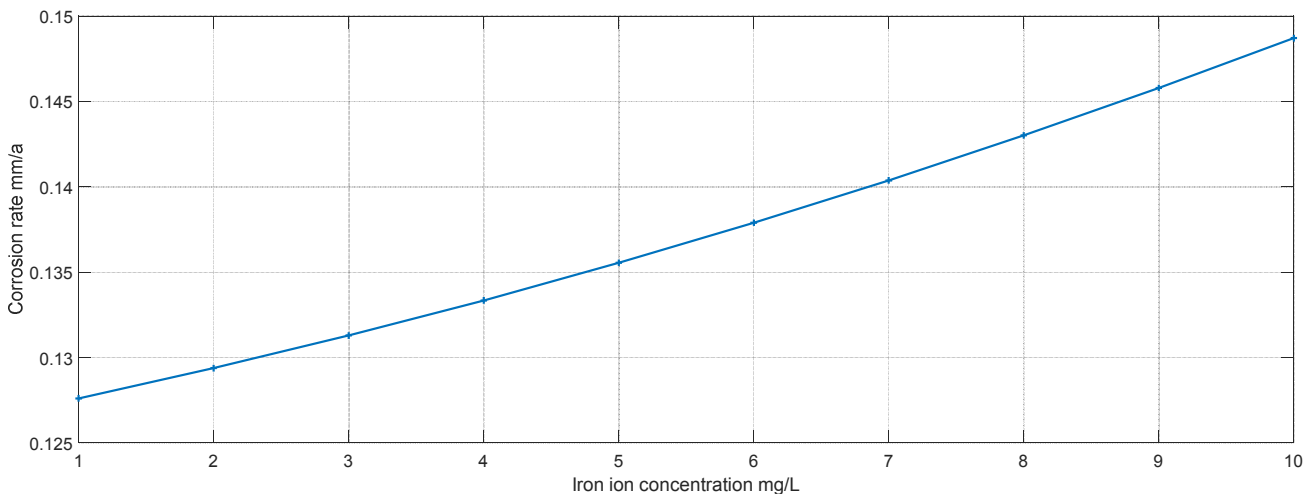


Figure 6. Effect of Iron Ion Concentration on Corrosion Rate.

5.2. Effect of pH Value on Corrosion Rate

pH value directly affects the concentration of HCl in water, As the pH increases, the concentration of H^+ decreases, and the reduction of hydrogen atoms decreases, so the corrosion rate decreases [17]. Similarly, the increase of pH value and the increase of OH^- concentration make the oxidation rate of iron

The iron ion in the sewage at the top of atmospheric pressure tower is the product of corrosion of the pipeline in the tower top equipment. Increased iron ion concentration indicates increased corrosion rate at the top of the pipeline. The higher the iron ion concentration, the more severe the corrosion of the pipeline [16].

First, pH value was kept at 8, chloride concentration was 30 mg/L, sulfide concentration was 30 mg/L, and the concentration of iron ion increased from 1 mg/L to 10 mg/L. The effect of iron ion concentration on corrosion rate is shown in Figure 6. Can be seen from Figure.6, The higher the ferric ion concentration, the greater the corrosion rate, in line with the natural law of corrosion. However, the corrosion rate is too small as the single variable increases, It may be that most of the selected data samples are within the normal range. The change of corrosion rate is relatively small, which leads to a smaller change of corrosion rate when the single variable exceeds normal range. In practice, the test data is within a reasonable range, and the model still has high accuracy in predicting the corrosion rate.

decrease, so the corrosion rate decreases. Maintain ferric ion concentration of 3 mg/L, chloride concentration of 30 mg/L, and sulfide concentration of 30 mg/L, gradually increasing the pH from 1 to 14. The effect of pH value on the corrosion rate is shown in Figure 7. From Figure 7, it can be seen that as the pH value increases, the corrosion rate gradually decreases.

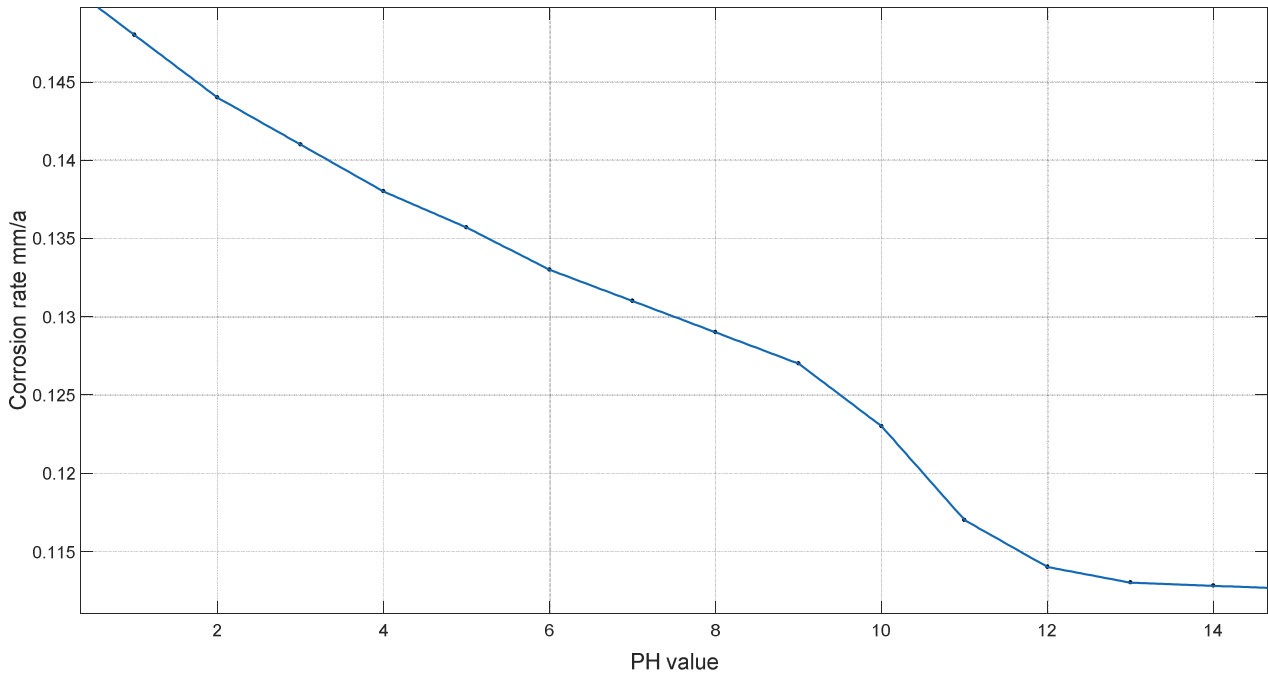


Figure 7. Effect of pH value on the corrosion rate.

5.3. Effect of Chloride Ion Concentration on Corrosion Rate

Under normal circumstances, the chloride ion concentration is in the range of 0-100 mg/L. As the concentration of chloride ions increases, the conductivity of the solution increases, and the H^+ concentration in the solution increases, preventing the formation of oxide films and accelerating corrosion rate [18].

Keep the pH at 8, ferric ion concentration 3 mg/L, sulfide concentration 30 mg/L, and gradually increase the chloride ion concentration from 10 mg/L to 100 mg/L. Chloride ion concentration on the corrosion rate shown in Figure 8. It can be seen from Figure 8 that as the concentration of chloride ions increases, the corrosion rate gradually increases.

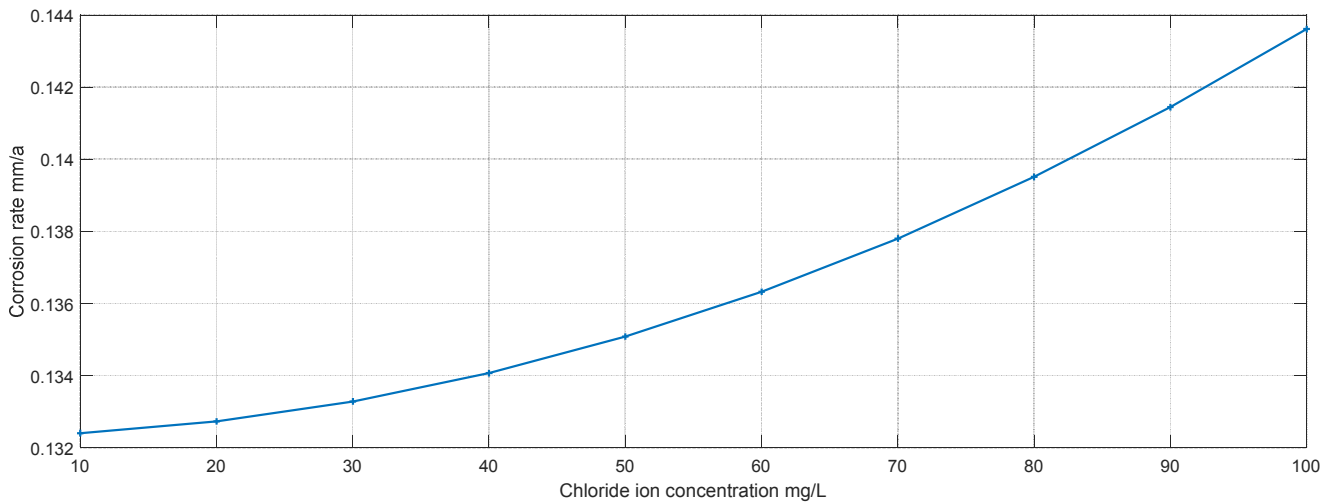


Figure 8. Effect of chloride ion concentration on corrosion rate.

5.4. Effect of Sulfide Concentration on Corrosion Rate

With the increase of sulfide concentration, it acts as a catalyst to participate in the oxidation of iron, and the corrosion of carbon steel is intensified [19]. Keep the pH at 8, ferric ion concentration 3 mg/L, chloride ion concentration 30

mg/L, and gradually increase the sulfide concentration from 10 mg/L to 100 mg/L. The effect of sulfide concentration on the corrosion rate is shown in Figure 9. As can be seen from Figure 9, as the sulfide concentration increases, the corrosion rate gradually increases.

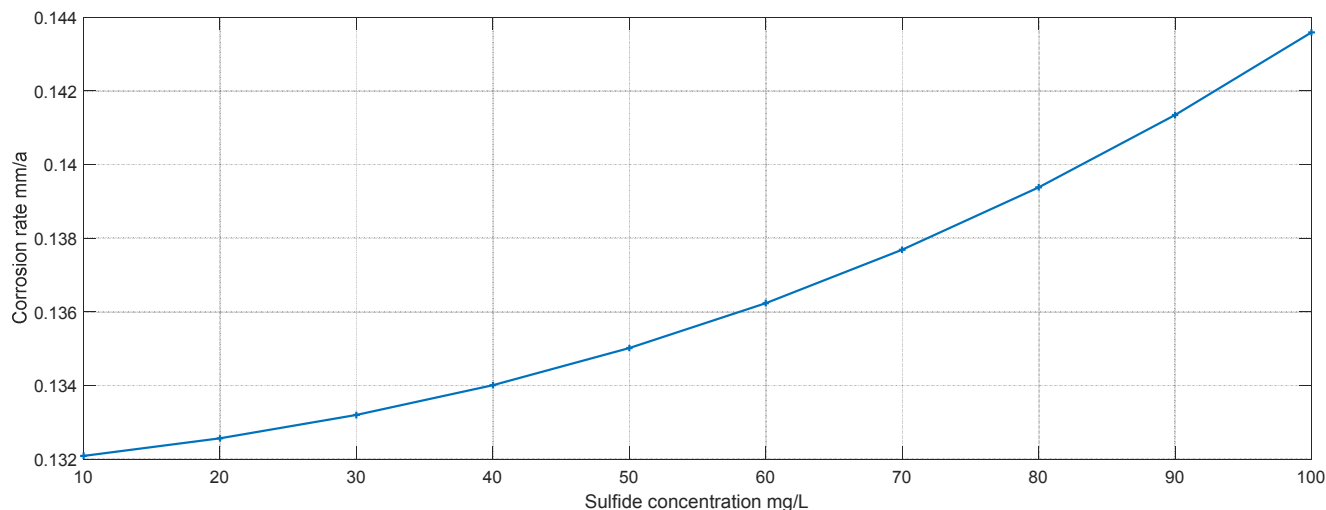


Figure 9. Effect of Sulfide Concentration on Corrosion Rate.

6. Conclusion

In this paper, the corrosion prediction model of naphtha and gas system at the top of the atmospheric tower is established by using the strong self-learning ability of BP neural network and the ability of multi factor synergy combined with the actual production situation. Genetic algorithm is used to optimize the prediction model and get a high prediction accuracy. Through the single factor investigation of the established model, it is confirmed that chloride ion concentration and sulfide concentration can accelerate the corrosion rate, Increase the pH of wastewater to inhibit the corrosion rate, An increase in iron ion concentration indicates an increase in the corrosion rate. It is proved that the established model has certain reference value for the corrosion research of low temperature part of atmospheric vacuum distillation unit, It has a certain guiding significance for the corrosion detection in actual projects.

Acknowledgements

Thanks to my leader Guangting Xue for his work on Corrosion research. Thanks to my colleague Guoming Yang for his work on English translation. Thanks to the other team members for their experimental work.

References

- [1] Feng W, Yang S. Thermomechanical processing optimization for 304 austenitic stainless steel using artificial neural network and genetic algorithm [J]. *Applied Physics A*, 2016, 122(12):1018.
- [2] Coban R (2013) A context layered locally recurrent neural network for dynamic system identification. *Eng Appl Artif Intell* 60(9):30–52.
- [3] Wranglen G. AN INTRODUCTION TO CORROSION AND PROTECTION OF METALS [J]. *Journal of Nuclear Medicine Official Publication Society of Nuclear Medicine*, 2016, 9(2):71-71.
- [4] Okonkwo P C, Sliem M H, Shakoor R A, et al. Effect of Temperature on the Corrosion Behavior of API X120 Pipeline Steel in H₂S Environment [J]. *Journal of Materials Engineering & Performance*, 2017(4):1-9.
- [5] R. Rahgozar, Remaining capacity assessment of corrosion damaged beams using minimum curves. *J. Constr. Steel Res.* 65, 299–307 (2009).
- [6] Shi X L. Development and Application of Artificial Neural Network [J]. *Journal of Chongqing University of Science & Technology*, 2006.
- [7] JOHN H K. Two Data Sets of near Infrared Spectra [J]. *Chemometrics and Intelligent Laboratory System*, 1997, 37:255-259.
- [8] Banu P S N, Rani S D. Knowledge-based artificial neural network model to predict the properties of alpha+ beta titanium alloys [J]. *Journal of Mechanical Science & Technology*, 2016, 30(8):3625-3631.
- [9] HOEIL C, HYESEON L, CHI-HYUCK J. Determination of Research Octane Number Using NIR Spectral Data and Ridge Regression [J]. *Bull Korean Chem Soc*, 2001, 22 (1):30-42.
- [10] Hanmaiahgari P R, Elkholy M, Riahi-Nezhad C K. Identification of partial blockages in pipelines using genetic algorithms [J]. *Sādhanā*, 2017, 42(9):1543-1556.
- [11] Rahmanifard H, Plaksina T. Application of artificial intelligence techniques in the petroleum industry: a review [J]. *Artificial Intelligence Review*, 2018(5):1-24.
- [12] Pol HH, Bullmore E (2013) Neural networks in psychiatry. *Eur Neuropsychopharmacol* 23(1):1–6
- [13] Paul S, Mondal R. Prediction and Computation of Corrosion Rates of A36 Mild Steel in Oilfield Seawater [J]. *Journal of Materials Engineering & Performance*, 2018:1-10.
- [14] Lai B-Q, Wang J-M, Duan J-J et al (2013), the integration of NSC-derived and host neural networks after rat spinal cord transection. *Biomaterials* 34(12):2888–2901.
- [15] Irani R, Nasimi R (2011) Application of artificial bee colony-based neural network in bottom hole pressure prediction in underbalanced drilling. *J Pet Sci Eng* 78(1):6–12.

- [16] Zhang L, Li H X, Shi F X, et al. Environmental boundary and formation mechanism of different types of H₂S corrosion products on pipeline steel [J]. 2017, 24(4):401-409.
- [17] Kermani M, Morshed A (2003) Carbon dioxide corrosion in oil and gas production—a compendium. *Corrosion* 59(8):659–683.
- [18] Akbar A. et al (2012) *Corrosion 2012*. NACE International.
- [19] Tanupabrunsun T, Brown B, Nestic S (2013) Effect of pH on CO₂ corrosion of mild steel at elevated temperatures. In: *Corrosion 2013*. NACE International.